Available online at www.sciencedirect.com
ScienceDirect
Biosensors and Bioelectronics 22 (2007) 2127–2131
BIOSENSORS & BIOELECTRONICS
www.elsevier.com/locate/bios

Uncoated quartz resonator as a universal biosensor

T. Yakhno [a,b,*], A. Sanin [a,b], A. Pelyushenko [a], V. Kazakov [a], O. Shaposhnikova [a], A. Chernov [a], V. Yakhno [a,b], C. Vacca [b], F. Falcione [b], B. Johnson [b]

[a] *Nonlinear and Optical Division of the Institute of Applied Physics RAS, 46 Ulyanova Street, GSP-120, 603950 Nizhny Novgorod, Russia*
[b] *Aria Analytics Inc., 1768 East 25th Street, Cleveland, OH 44114, USA*

Received 21 April 2006; received in revised form 13 September 2006; accepted 27 September 2006
Available online 13 November 2006

Abstract

We studied dynamic processes in drying drops of model protein–salt solutions, using an uncoated quartz resonator as a biosensor. To measure these processes we developed a method based on recording the dynamics of the Acoustic-Mechanical Impedance (AMI) of a drop as it dried on the surface of a quartz resonator oscillating at a resonant frequency of 60 kHz. The aim of this work was to highlight the role of some components of serum in self-organization processes. Human serum albumin (HSA), fibronectin (Fn), immunoglobulin G (IgG), immunoglobulin M (IgM), bovine serum albumin (BSA), sodium chloride (NaCl), Potassium Chloride (KCl), and nonionic surfactant $O(CH_2CH_2)_nCH_2CH_2OH$ were used as components of the tested solutions.

It was shown that dynamics of the AMI in drying drops were closely related to liquid composition. This approach allowed us to distinguish with good accuracy solutions in which one or more components (proteins or salts) were replaced by other components with the same mass concentration. We assumed that these differences were due to different surface properties and native functions of proteins, and different positions of salts in the Hofmeister line. Our preliminary work demonstrated that the dynamics of phase transitions in drying drops of serum could be used as an informative parameter for medical diagnostics. In this study, we highlight some positions in this cause-effect chain.

Keywords: Quartz sensors; Drying drops; Dynamics of phase transitions

1. Introduction

Quartz Crystal Microbalance (QCM) sensors are widely used to perform medical diagnostic testing of biological liquids. These sensors have coatings that selectively bind specific chemicals or structures. This binding affects the acoustic properties of the liquid such as velocity, attenuation and frequency. Based on this approach, rapid detection of fibrinogen and fibrin degradation products was developed (Aizawa et al., 2004); bacteria, immunoglobulins, and C-reactive protein were detected (Muramatsu et al., 1989; Chue et al., 1996); QCM was used to identify different human blood cells (Konig and Gratzel, 1993a, 1993b). Also, QCM sensors with special coatings can be used as gas-sensors (Zhou et al., 1994; Lazarova et al., 1996). Uncoated QCM sensors are commonly used for mass measuring in static and dynamic conditions (Gomes, 2001; Yamasaki et al., 2004). The measured frequency shift is proportional to the mass of the deposited film, so the sensor provides thickness data by measuring the film density and acoustic impedance. Another utilization of QCM sensors is measuring viscosity of liquids (Martin and Ricco, 1987).

In contrast to this approach, we use temporal self-organization processes in drying drops as an informative parameter for liquid identification, and an uncoated quartz resonator to sense these processes (Yakhno et al., 2002a, 2003). A drying drop of liquid on a solid substrate is a natural model of a self-organizing system. There are many variants of the drying processes such as drop volume, environment, substrate properties, and liquid composition (Deegan, 2000; Deegan et al., 2000). Thus, if we control all parameters except liquid composition, only this parameter will be responsible for self-organizing processes in the drying drop. Self-organizing processes in drying protein solutions were first reported by Rapis (Rapis, 1988). Shabalin and Shatokhina used this phenomenon in medical diagnostics (Shabalin and Shatokhina, 2001).

* Corresponding author at: Nonlinear and Optical Division of the Institute of Applied Physics RAS, 46 Ulyanova Street, GSP-120, 603950 Nizhny Novgorod, Russia. Tel.: +7 8312 169 594; fax: +7 8312 363 792.
E-mail address: tanya@awp.nnov.ru (T. Yakhno).

0956-5663/$ – see front matter © 2006 Elsevier B.V. All rights reserved.
doi:10.1016/j.bios.2006.09.029

We showed that it is possible to get information not only from the morphology of dried drops, but also from dynamic parameters (Yakhno et al., 2002b). As a drop dries on the surface of a quartz resonator, the drop self-organization is represented by the dynamics of phase transitions that are recorded using variation in the Acoustical-Mechanical Impedance (AMI). Our earlier studies report the utility of this approach in medical diagnostics (Yakhno et al., 2005).

Earlier we showed that the drop drying process of serum begins with phase transitions of proteins, and the protein phase perturbations are completed at the formation of a gel matrix (Yakhno et al., 2004). The final stage of drop drying involves salt crystallization in the residuals of liquid phase immobilized into the gel. The kinetics of water evaporation during the phase transitions of salts is determined by physical properties of the gel, thus, it can characterize the liquid as a whole. It was also established that the dynamics of AMI signal variation reflects the sequential stages of structure formation in a drying drop, and can be used for their description.

Because, some diseases are accompanied by increased concentrations of immunoglobulins, and varying levels of Fn in serum (Heil et al., 1999), we wanted to study the shape of the AMI curves resulting from variation of these serum components in an HSA solution. The aim of this work was to trace causal relationships responsible for diagnostic data by controlling the concentration of these serum proteins in model protein–salt solutions.

2. Materials and methods

2.1. Description of the technology

A 5 microliter drop of test liquid was dried on the surface of a quartz resonator oscillating at a constant ultrasonic frequency. This frequency agreed with the resonant frequency of the unstrained resonator. We examined the shear characteristics of a drop, which were extremely sensitive to the occurrence and rise of new-phase structures. The measured quantity was the dynamic-complex conductance of the resonator, which was converted to the Acoustic-Mechanical Impedance of the drying drop, and the drying dynamics were displayed in the form of a curve. As the sensitive element, we used a resonator in the form of a rectangular plate of quartz XYS/1°30′ with section 48.0 by 4.5 by 1.0 mm. A drop of liquid that had been under normal room conditions (T = 18–22 °C, P = 740–760 mmHg, and H = 60–70%), was placed onto the operational portion of the resonator using a micropipette, and the AMI recorded and displayed in real time. The sample was covered to protect against external streams of air. Proprietary software made it possible to follow the dynamics of the measured quantities in real time on the display. When recording was complete, the results were saved to a database. After the measurement procedure, the operating surface of the quartz plate was washed carefully with distilled water, ethanol and then carefully dried. A control solution of 7% bovine serum albumin in a physiologic saline solution was run daily to standardize device performance.

To determine variation in the solutions tested, we mathematically deconstructed each set of curves and parameterized the observed differences. From these data we developed "Shape Indices" (SI) for the AMI curves. These parameters allowed us to represent different liquids by numerical values with statistical distinction ($M \pm \sigma$). All samples under comparison were tested under the same laboratory conditions. Device construction and the measuring procedure are described in more detail (Yakhno et al., 2003, 2005).

2.2. Liquids under study

Protein–salt solutions were prepared using either lyophilized bovine serum albumin (BSA, 68 kDa) or human serum albumin (HSA, 67 kDa) in distilled water or salt-in-water solutions. Albumins were purchased from Sigma (USA). Salts (NaCl, KCl) were labeled "chemically pure" ("Reaktiv Inc.", Russia). Other human serum proteins studied were obtained from "IMTEK, Ltd." (Russia): immunoglobulin G (IgG, 150 kDa), immunoglobulin M (IgM, 900 kDa), and fibronectin (Fn, 420 kDa). All solutions were prepared a day prior to experimentation, refrigerated overnight and allowed to come to room temperature before testing.

Protein content in human serum model solutions varied from 70 to 86.4 g l^{-1}. This coincides with the normal total protein concentration in human serum (Heil et al., 1999). Each protein mix had a corresponding HSA control solution of the same protein mass (Table 1) and was dissolved in physiological NaCl solution (9.0 g l^{-1}). As a nonionic surfactant, we used $O(CH_2CH_2)_nCH_2CH_2OH$. Every protein variation was tested not less than 10 times. Table 1 below summarizes the protein content of the protein–salt samples.

3. Results and discussion

Typical shapes of the AMI curves of protein–salt solutions are represented at Fig. 1. The initial part of the curve (up to

Table 1
Protein content in protein–salt solutions

No.	Protein composition	[Total protein] (g l^{-1})	[HSA] (g l^{-1})	[Fn] (g l^{-1})	[IgG] (g l^{-1})	[IgM] (g l^{-1})
1	HSA	70	70	–	–	–
2	HSA + Fn	70.4	70	0.4	–	–
3	HSA + Fn + IgG	86.4	70	0.4	16	–
4	HSA (control 1)	86.4	86.4	–	–	–
5	HSA + Fn + IgG + IgM	84.5	70	0.3	12	2.2
6	HSA (control 2)	84.5	84.5	–	–	–

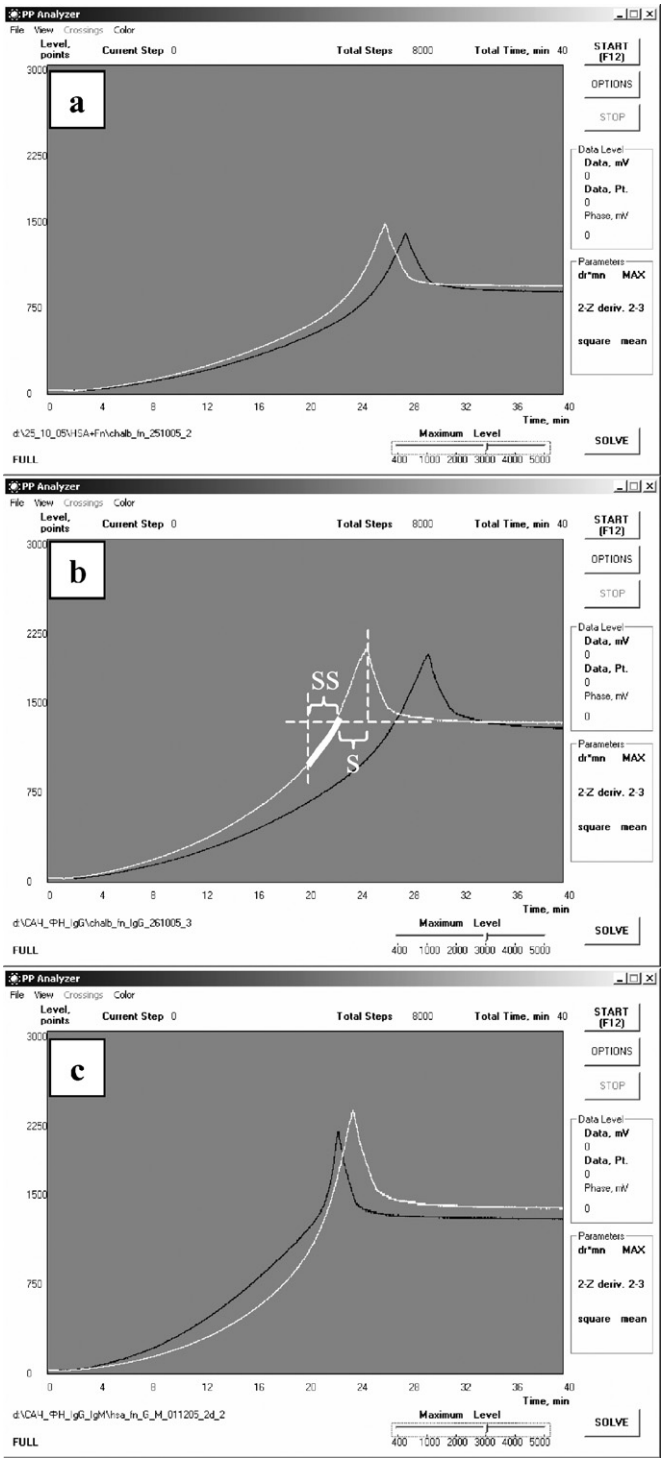

Fig. 1. Comparison of HSA solutions containing various human proteins in each case the *X*-axis is time (min), and *Y*-axis is AMI (calculated units). Protein–salt solutions described in Table 1: (a) HSA (black), HSA + Fn (white); (b) control 1 (black), HSA + Fn + IgG (white); (c) control 2 (black), HSA + Fn + IgG + IgM (white). In (b), the portion "S" is equal with the time of salt crystallization. The portion "SS" is the mirror image of portion S. Shape Index 1 was calculated using these areas as averaged derivative of the highlighted segment of the curve.

Table 2
Shape Index value for the AMI curves of protein–salt solutions

Protein solution	Shape Index 1 ($M \pm \sigma$)
HSA	12.0 ± 0.1
HSA + Fn	10.9 ± 0.4
HSA + Fn + IgG	16.6 ± 0.8
HSA (control 1)	13.3 ± 0.3
HSA + Fn + IgG + IgM	23.7 ± 1.2
HSA (control 2)	13.4 ± 0.5

horizontal dashed line at Fig. 1b) corresponds to protein phase transitions and gel matrix formation followed by the beginning of crystallization then the descending portion of the curve represents evaporation of residuals of free water. The right (constant) part of the AMI curve reflects dried mass residuals with film water.

Adding the micro quantity of Fn to the HSA salt solution (Table 1) results in left shift of the AMI curve, and changes the geometry of saline peak. To formalize the changes in the shape of the AMI curves we used Shape Index 1 (in calculated units), which is based on the value of averaged derivative of the ascending part of the AMI curve. For every AMI curve this segment is determined as a time of salt crystallization (Fig. 1b, internal bracket (S)), which was placed to left (Fig. 1b, external bracket (SS)), so, measuring part of the curve was limited by the portion of the curve that is highlighted (heavy line) as it is shown in the picture.

In Fig. 1(b, c), we can see that HSA solutions contaning IgG, and IgG + IgM, differ in the shape of the AMI curves compared to their corresponding control solutions that contained only HSA (Table 1). It is interesting that adding Fn to HSA led to decrease in Shape Index 1, whereas substituting a portion of the HSA with the same mass of immunoglobulins in the solution led to an increase of Shape Index 1 (Table 2). Fibronectin is the most investigated glycoprotein of intercellular martix (Nikolaev, 1998). It participates in reparation processes in tissues by forming a net, which provides support for the cells occupying a wound area. Fibronectin also plays an important role in opsonization of bacteria (Gilot et al., 1999). The decreasing value of Shape Index 1 after Fn adding in our experiments represents a slower salt crystallization process occuring in the HSA + Fn solution as compared to the HSA control. We suggest that this phenomenon is a result of protein consolidation at the drop-air border due to Fn net formation and Fn in the drying drop can manifest its native function.

It is known that extension in size of surfactant molecule by one CH_2 – unit, increases its surface energy in 3–3.5 times, simultaneously its solubility in water decreases proportionally (Tchukin, 2004). Thus, we can list serum proteins based on their increasing surface activity; HAS–IgG–Fn–IgM. It signifies that immunoglobulins and Fn in drying drops must occupy the upper position, and act similarly on water evaporation during drying. Because immunoglobulins have no mechanical function in blood, in drying drop they conduct themselves as proteins with high surface energy, and settle on the drop-air border, lowering suface tension. This action leads to

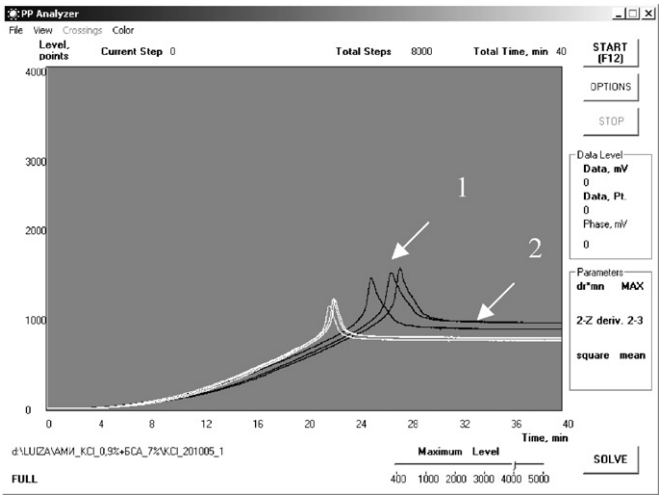

Fig. 2. NaCL vs. KCl in BSA Solution. *X*-axis is time (min), and *Y*-axis is AMI (calculated units). AMI curves of drying drops of protein–salt solutions: BSA + NaCl (black); BSA + KCl (white). "1" is maximum height of the salt peak; "2" is the level at which equilibrium is reached.

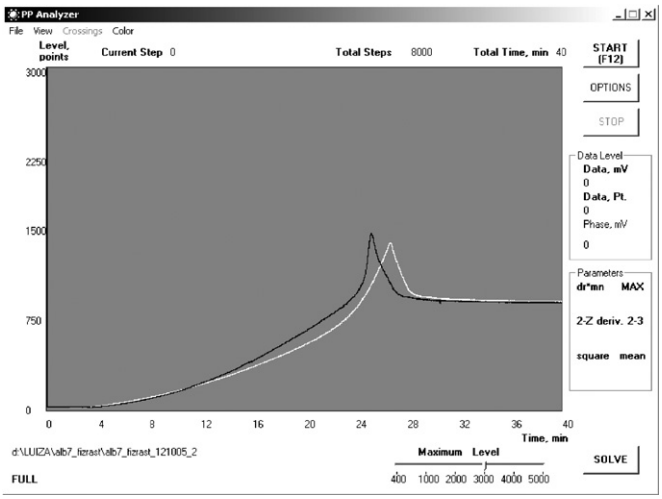

Fig. 3. BSA vs. HSA AMI Curves. *X*-axis is time (min), and *Y*-axis is AMI (calculated units). AMI curves of drying drops of protein–salt solutions BSA (black); HSA (white).

increased area between the drop and the quartz plate, and causes accelerated water evaporation and salt crystallization processes occur more rapidly (i.e., Shape Index 1 decreases). The lowering in surface tension of HSA solutions after addition of immunoglobulins, as well as rise in surface tension after adding Fn, were shown by direct measurement (Yakhno et al., 2006).

We also tested BSA solutions (70 g l^{-1}) in NaCl or KCl water solutions (9 g l^{-1}) and demonstrated that replacement of NaCl with KCl in the BSA solution led to manifest changes in the AMI dynamics as the drop dried (Fig. 2). These differences were due to Na^+ and K^+ ion features, and their positions in the Hofmeister line, in accordance with their ability to salt-out proteins from solutions and to increase surface tension on the phase borders (Muschol and Rosenberger, 1995, 1997; Curtis et al., 1998). Despite the fact that both solutions had the same protein/salt mass ratio, their initial ionic strength (I) was differerent: I(NaCl) = 0.08, and I(KCl) = 0.06. We believe that the ion charge and size play a significant role in the initialization and developing protein phase transitions in drying drops of protein solutions. Parametrization of the AMI curves by means of Shape Index 6 demonstrated these differences in a digital form. Shape Index 6 is based on the maximum AMI of the salt peak (Fig. 2, 1), the level of the right part of the curves (Fig. 2, 2), and geometry of saline peak. For BSA + NaCl Shape Index 6 was equal 514.7 ± 40.4, and for BSA ± KCl it was 324.5 ± 19.0.

The next series of experiments were aimed at tracing differences in drop drying processes when BSA or HSA (70 g l^{-1}) were dissolved in physiologic NaCl solution (Fig. 3). We calculated Shape Index 1, which was equal to 8.7 ± 0.5, and 12.0 ± 0.1 for BSA and HSA solutions, respectively. Also, we applied Shape Index 3 to the HSA–BSA experiments. This index is based on the value of the difference between averaged derivative of the descending and ascending parts of saline peak of the AMI curve from its maximum to the constant the AMI value level. Shape Index 3 was 46.7 ± 1.8 for BSA, and 11.1 ± 0.6 for HSA solutions.

Thus, we can conclude that in drying drops of HSA salt solution, salt crystalization is a slower process than in BSA. We suggest that these distinctions are governed by the differences in molecular shape, as well as discharge value and distribution around them (Chang and Bae, 2003). These serum protein features influence properties of the protein gel formed during drying and also the water diffusion through it during the final stages of the drop drying process.

In our final experiments, we examined the effects of the addition of a surfactant to a BSA solution. It has been reported that the surfactant replaces protein from the adsorptive layers resulting in a lowering of the surface tension of the system

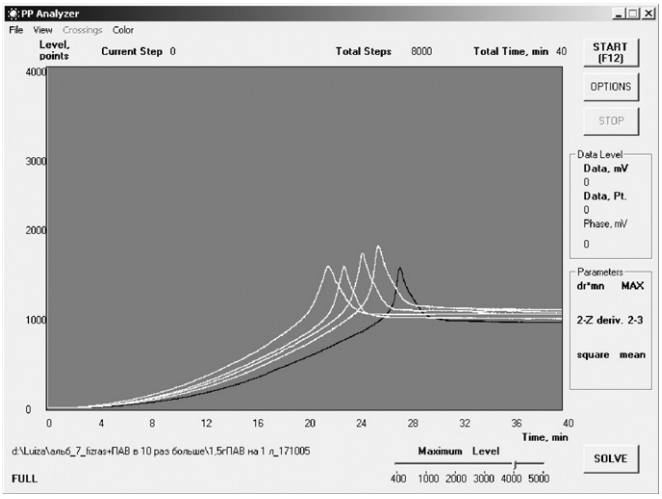

Fig. 4. Effects of surfactant addition. *X*-axis is time (min), and *Y*-axis is AMI (calculated units). AMI curves of BSA solution and the addition of surfactant: BSA 70 g l^{-1} in [NaCl] 9 g l^{-1} solution without surfactant (black); addition of nonionic surfactant (white) surfactant concentration from right to left: 0.20 g l^{-1}; 0.50 g l^{-1}; 1.00 g l^{-1}; 1.50 g l^{-1}.

(Joos and Serrien, 1999). Ionic and nonionic surfactants have some differences in their action, but their main influence on the solutions is the same (Mackie et al., 2000; Gunninh et al., 2004). The addition of a nonionic surfactant to BSA salt solution stimulates the dose-dependent left shift of the AMI curves of drying drops (Fig. 4). Our microscopic investigations demonstrated that addition of surfactant reduces clustering of colloidal particles and gelation. Most strikingly, the addition of this surfactant systematically reduced the time required for the beginning of NaCl crystallization. The degree of drop cracking intensified with increase in surfactant concentration. Furthermore, cracks formed earlier in the drop drying process. These changes are due to a gradual decrease of surface energy on the drop-air border eases water diffusion through the adsorbtive layer causing evaporation to be intensified. Because water is a plasticizer, its evaporation increases the fragility of the system, and leads to the earlier and more intensive cracking of drying drops as the surfactant concentration increases. This dependence becomes apparent when we look at the AMI curves.

4. Conclusions

We have shown that the use of the uncoated quartz resonator makes it possible to distinquish, with good accuracy, differences in protein–salt solutions including samples that mimic human serum. The main feature of this approach was that phase transitions in drying drop were registered and used as the informative parameter. Immunoglobulins and Fn act in opposite ways on the drop drying and this can be explained by their different native functions in blood. Our methodology is also a measurement of numerical differences between solutions containing different proteins and salts of the same weight concentrations. We demonstrated that the drop drying process is significantly influenced by addition of surfactant. The data presented support the application of our approach to medical diagnostics, industrial applications, and various other areas.

Acknowledgements

The authors are very grateful to Dr. A. Babin for productive discussion of our results.

References

Aizawa, H., Kurosawa, S., Tozuka, M., Park, J.-W., Kobayashi, K., 2004. Sens. Actuators B 101, 150–154.
Chang, B.H., Bae, Y.C., 2003. Biophys. Chem. 104, 523–533.
Chue, X., Jiang, J., Shen, G., Yu, R., 1996. Anal. Chim. 336, 185–193.
Curtis, R.A., Prausnitz, J.M., Blanch, H.W., 1998. Biotechnol. Bioeng. 57, 11–21.
Deegan, R.D., 2000. Phys. Rev. E 61 (1), 475–485.
Deegan, R.D., Bakajin, O., Dupont, T.F., Huber, G., Nagel, S.R., Witten, T.A., 2000. Phys. Rev. E 62 (1), 756–765.
Gilot, P., Andre, P., Content, J., 1999. Infect. Immun., 6698–6701.
Gomes, M.T.C.R., 2001. Curr. Top. Anal. Chem. 2, 187–193.
Gunninh, P.A., Mackie, A.R., Gunninh, A.P., et al., 2004. Biomacromolecules 5, 984–991.
Heil, W., Koberstein, R., Zawta, B., 1999. Reference Ranges for Adults and Children. Pre-analytical Considerations. Roche Diagnostics GmbH, Mannheim.
Joos, P., Serrien, G., 1999. J. Colloid Interface Sci. 145, 291–294.
Konig, B., Gratzel, M., 1993a. Anal. Chim. Acta 281, 13–18.
Konig, B., Gratzel, M., 1993b. Anal. Chim. Acta 276, 229–233.
Lazarova, V., Spassov, L., Gueorguiev, V., Andreev, S., Malonov, E., Popova, L., 1996. Vacuum 47 (12), 1423–1425.
Mackie, A.R., Gunninh, A.P., Wilde, P.J., et al., 2000. Langmuir 16, 8176–8181.
Martin, S.J., Ricco, A.J., 1987. Appl. Phys. Lett. 50, 1474–1476.
Muramatsu, H., Tamita, E., Karube, I., 1989. J. Membr. Sci. 41, 281–290.
Muschol, M., Rosenberger, F., 1995. J. Chem. Phys. 103, 10424–10432.
Muschol, M., Rosenberger, F., 1997. J. Chem. Phys. 107, 1953–1962.
Nikolaev, A.Ya., 1998. Biological Chemistry. Medical Informative Agency, Moscow.
Rapis, E.G., 1988. Pis'ma v Zh. T. Ph. 14 (17), 1560–1565.
Shabalin, V.N., Shatokhina, S.N., 2001. Morphology of Biological Fluids. Khrisostom, Moscow.
Tchukin, E.D., 2004. Colloid Chemistry. High School, Moscow.
Yakhno, T.A., Yakhno, V.G., Sanin, A.G., Shmelev, I.I., 2002a. Biophysics 47 (6), 1101–1105.
Yakhno, T.A., Yakhno, V.G., Levin, G.Ya., Korochkina, O.V., Buzoverya, M.E., 2002b. In: Uvarova, L.A. (Ed.), Proceedings of the IVth International Conference on Mathematical Modeling. Moscow, vol. 2, pp. 265–275.
Yakhno, T.A., Yakhno, V.G., Sanin, A.G., Sanina, O.A., Pelyushenko, A.S., 2003. In: Rodrigues-Vazquez, A., Abbott, D., Carmona, R. (Eds.), Bioengineered and Bioinspired Systems. Proc. SPIE. Spain, vol. 5119, pp. 87–99.
Yakhno, T.A., Yakhno, V.G., Sanin, A.G., Sanina, O.A., Pelyushenko, A.S., 2004. Tech. Phys. 49 (8), 1055–1063.
Yakhno, T., Yakhno, V., Sanin, A., Egorova, N., Terentiev, I., Smetanina, V., 2005. IEEE Eng. Med. Biol. Mag. 24 (2), 96–104.
Yakhno, T., Kazakov, V., Sanin, A., Shaposhnikova, O., Chernov, A., 2006. Tech. Phys., in press.
Yamasaki, A., Cunha, M.A.S.D.A., Oliveira, J.A.B.P., Duarte, A.C., Gomes, M.T.S.R., 2004. Biosens. Bioelectron. 19, 1203–1208.
Zhou, R., Vaihinger, S., Geckeler, K.E., Gopel, W., 1994. Sens. Actuators B 19 (1–3), 415–420.